Dewetting of Thin Polymer Films

Günter Reiter
Max-Planck Institute for Polymer Research, P.O. Box 3148, 6500 Mainz, Federal Republic of Germany
(Received 27 August 1991)

Thin polystyrene films (< 100 nm) on silicon substrates undergo dewetting when annealed above the glass transition temperature. Three different stages can be distinguished: The smooth films break up by the creation of cylindrical holes. The holes then grow and form rims ahead of them which finally contact each other creating "cellular" structures. The rims are unstable and decay into droplets. The influence of the film thickness on this process is investigated and compared to recent theoretical predictions of spinodal decomposition of partially wetting thin films.

PACS numbers: 68.15.+e, 47.20.−k, 68.45.−v

Thermal stability of thin polymer films against shape changes is of technological importance to applications like coatings or dielectric layers. Thin films are also used for the investigation of fundamental problems of polymer diffusion [1] or adsorption [2]. For these purposes smooth and stable surfaces and interfaces are required. Using techniques like spin coating, polymer films can be prepared even on nonwettable surfaces. However, such films are not stable. Above the glass transition temperature they will break up [3,4] and will dewet the substrate, i.e., the films are transformed into droplets. In contrast to spreading or wetting of liquids on solid surfaces [5–7], little is presently known about the opposite process of drying or dewetting [8,9]. An experimental study of the dynamics of dewetting of thick films has been recently reported [10]. These films are metastable and dewetting proceeds via nucleation. In our experiments we use thin films (< 100 nm) which are unstable and spinodal decomposition is expected to play a role. van der Waals forces are relevant and the process is very sensitive to the film thickness [8]. Although dewetting will occur for any liquid on a nonwettable surface, the use of polymers in this context has two advantages. The vapor pressure of polymers is negligible and thus the mass of the film is conserved. The low mobility of polymers favors time-resolved experiments.

Following the initiation of dewetting the smooth films break up. The resulting holes grow and finally form almost regular structures. Such patterns are of interest because of their prevalence in many fields such as physics, biology, etc. For example, similar structures can be found in plants, soap froths, crack patterns in the soil of deserts, etc. Cellular structures represent a compromise between order and chaos [11,12].

For the experiments we used silicon substrates which were supplied by Wacker Chemitronics, Federal Republic of Germany. Two different nonwettable surfaces (type *A* and type *B*), as obtained from the supplier, were used [13]. For the polymer films we used polystyrene (M_w =28000 g/mol, $M_w/M_n < 1.05$) purchased from Polymer Laboratories, United Kingdom. Thin films were prepared by spin coating a toluene solution of the polymer onto the silicon substrates. The film thickness was determined by x-ray reflectometry with an accuracy of 0.1–0.2 nm [14]. The surface homogeneity was checked with a commercial optical phase interference microscope (OPIM, Maxim 3D, ZYGO Corp., U.S.A.). Dewetting took place when the films were annealed in a vacuum oven for different times at temperatures above the glass transition. The samples were then quenched down to room temperature and examined again by OPIM. Contact angles (Θ) which are a measure of the wettability [6,15] as determined by OPIM [16] were $22° \pm 4°$ and $42° \pm 5°$ for wafers of type *A* and *B*, respectively. This qualitative distinction between the wafers is sufficient for the purpose of the present study.

Experiments were performed in two different ways. In the first mode, two series of samples were annealed at 166 °C for 12 h [17]. Typical pictures are shown in Fig. 1. The droplets in Fig. 1 are not randomly distributed but form rather regular patterns. In the second series of experiments samples on wafers of type *A* were annealed for 15 min to 2 h at temperatures between 135 and 150 °C. These experiments aim to elucidate the initial stages of dewetting and the process which leads to the pattern formation. Some typical resulting pictures are shown in Fig. 2. When the defects are large enough to be detected by a light microscope randomly distributed holes are seen. Their depth relative to the unperturbed film surface was determined by using the analysis program of the OPIM. Within experimental errors ($\simeq$1 nm) the hole depth is identical with the initial film thickness. The holes grow and the removed matter is accumulated at the edges of the holes. A rim is formed with a cross section which is a portion of a circle. Eventually the holes become large enough, so that their rims contact each other. This results in the formation of unstable ribbons which decay into droplets of size proportional to the diameter of the ribbon [18,19]. The arrangement of the droplets resembles cellular structures. The growth process is slightly different for samples on wafers of type *B*. Droplets are formed while the holes are growing. Nevertheless, at the end, the rims merge and break up into droplets thus generating a comparable pattern of polygons as in the previous case.

It is obvious from the micrographs (see Fig. 1 and

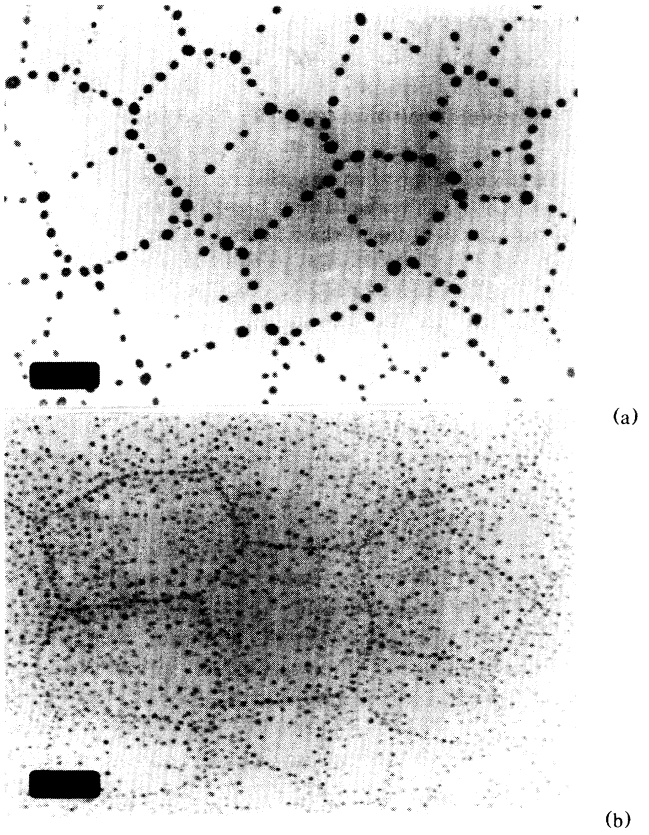

FIG. 1. Micrographs of the final stage of dewetting of 45-nm-thick polystyrene films on silicon wafers of (a) type A and (b) type B. The length of the bar is 100 μm.

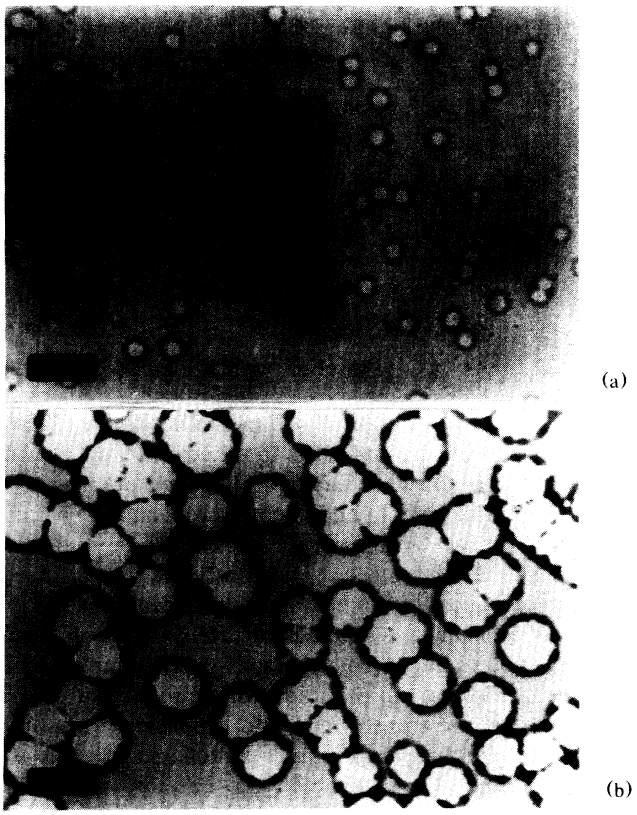

FIG. 2. Micrographs at different stages of dewetting of a 40.5-nm-thick polystyrene film on a silicon wafer of type A after (a) 20 min at 146 °C and (b) 120 min at 146 °C. The area between the holes has become rough during annealing as indicated by black spots on the micrographs [especially (a)]. The length of the bar is 100 μm.

[16]) that the diameter of the droplets (D_d), the number of droplets per reference area A (N_d), and the diameter of the polygons (D_P) depend on the thickness of the initial film (h). At least ten pictures of each sample taken at different parts of the sample were analyzed. The distributions of D_d, N_d, and D_P are found to be rather narrow. We use their averaged values for further purposes. Errors caused by this approximation are estimated to be about 15%. However, the errors may be larger because the results are sensitive to roughness of the substrate as well as inhomogeneities and defects of the films. The results of D_d, N_d, and D_P as a function h are plotted in Figs. 3 and 4. Power-law dependences are found and the corresponding exponents are given in Table I. An interesting feature is that D_P is independent of the type of wafer. In marked contrast D_d and N_d vary from surface to surface, both in absolute value and in the corresponding exponent.

For samples on wafers of type A we determined the number (N_H) of initial holes (hole diameter approximately 3 μm) per reference area A. Several samples of the same thickness were heated at the same temperature for different times. As long as the holes did not coalesce the number of defects was constant, and only the diameter of the holes increased. N_H as a function of film thickness is presented in Fig. 5. The data are compared with

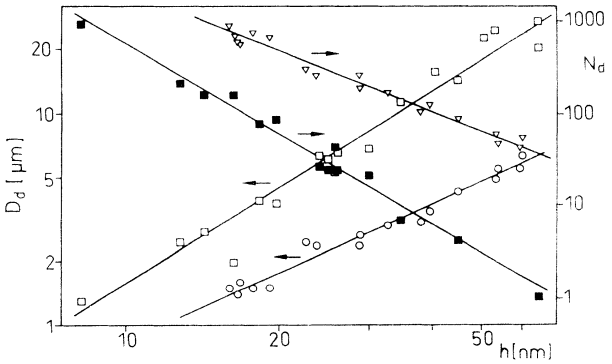

FIG. 3. Double logarithmic plot of the average diameter of droplets (D_d) and the average number of droplets per 10^4 μm^2 (N_d) as a function of film thickness (h). Samples on wafer of type A: □, D_d; ■, N_d; on wafers of type B: ○, D_d; ▽, N_d. The values of the slopes are given in Table I.

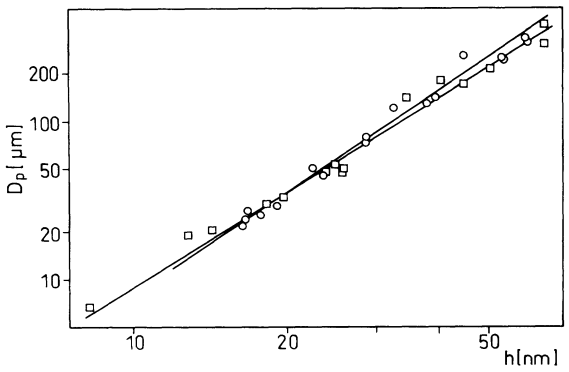

FIG. 4. Double logarithmic plot of the average diameter of polygons (D_P) as a function of film thickness (h). □, samples on type-A wafers; and ○, samples on type-B wafers. The values of the slopes are given in Table I.

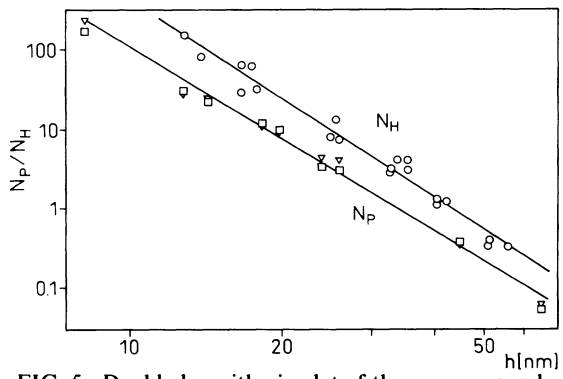

FIG. 5. Double logarithmic plot of the average number of initial holes per 10^4 μm^2 (N_H) as well as the average number of polygons per 10^4 μm^2 (N_P) as a function of film thickness (h) for samples on type-A wafers. ○, N_H, □, N_P directly measured, and ▽, N_P calculated by taking the inverse square of the polygon diameter. The values of the slopes are given in Table I.

the number of polygons per reference area (N_P) as determined by direct counting and the proportionality to D_P^{-2}. The number of initial holes is significantly higher than the number of polygons. The discrepancy is due to the coalescence of rims without formation of droplets at the early stages of hole growth. The material of the boundary is drained and a larger hole is formed. This process is responsible for the comparatively uniform size of the polygons. In its absence the random distribution of initial holes would persist and result in a large polydispersity of the polygon size. At this point it should be noted that also the size of the initial holes is rather uniform [compare Fig. 2(a)]. This suggests a nearly simultaneous breakup of the initially smooth film at the positions of the holes. Nucleation, e.g., by impurities or small defects is not likely because the probability to create a hole should not be limited to a narrow time regime and thus would lead to holes of different sizes. The above results show that we have to make a clear distinction between the processes of breakup of the film, which does not seem to depend on the wettability of the substrate, hole growth, and droplet formation.

The stability of thin films of nonvolatile liquids forced onto substrates which they partially wet only was theoretically considered by Brochard-Wyart and Daillant [8]. They assume surface modulations of the type $\xi(x,t) = h + u\exp(iqx)\exp(-t/\tau)$, with amplitude u, wave vector q, time t, relaxation time τ, and where x is a coordinate parallel to the surface. The perturbations of the surface induce a pressure gradient which, in turn, causes a Poiseuille flow [6,8]. We have competition between the Laplace pressure p_L [8], which depends on the ratio of surface tension and radius of curvature, and the disjoining pressure $\Pi(h)$ [6,20]. $\Pi(h)$ depends on h^{-3} (assuming nonretarded van der Waals forces) and tends to thicken and thus roughen the film while the flow induced by p_L flattens the film.

TABLE I. Exponents of the dependences of D_d, N_d, D_P, N_P, and N_H on film thickness resulting from Figs. 3–5.

Parameter	Wafer type A	Wafer type B
D_d	1.54 ± 0.08	1.05 ± 0.05
N_d	-3.26 ± 0.14	-2.11 ± 0.09
D_P	1.91 ± 0.07	2.06 ± 0.07
N_H	-4.10 ± 0.15	
N_P	-3.80 ± 0.14	

As long as τ is positive the perturbations are damped exponentially with time. However, τ may become negative causing an exponentially growing amplitude of the surface modulations for $q < q_c = 3a/h^2$ (a being a length of order of a monomer size). The central result of Ref. [8] is that films below a thickness of approximately 100 nm are unstable and break up via spinodal decomposition. The characteristic distance of the initial defects is proportional to h^2 and therefore the area per defect is proportional to h^4. Comparing this prediction with the exponent characterizing the dependence of N_H on film thickness (-4.10 ± 0.15) the agreement seems to be perfect. One may thus conclude that Ref. [8] describes the process of breakup adequately.

The experiments on type-A wafers show a relation between the size of the polygons and the diameter of the droplets. The following equation describes the conservation of mass: $D_P^2 h \sim D_P D_R^2 \Theta$, with D_R being the diameter of the ribbon formed when the rims get into contact. The measurements reveal $D_P \sim h^{1.91 \pm 0.07}$ and accordingly $D_R \sim h^{1.46 \pm 0.04}$. The ribbon is unstable and breaks into droplets of size D_d proportional to D_R [6,18,19]. The measured exponent of D_d as a function of h is 1.54 ± 0.08 in good agreement with the expected value. The size of the droplets can be determined independently via N_d. Again, requiring mass conservation the following relation has to be fulfilled: $Ah \sim N_d D_d^3 \Theta$. Using the experimen-

tally found exponent of -3.26 ± 0.14 for N_d as a function of h gives an exponent of 1.42 ± 0.05 for D_d. A different situation is found for type-B wafers. Droplets are formed before the rims meet. Accordingly, there is no correlation between the size of the polygons and the droplets.

The patterns formed by the droplets, especially on wafers of type A, are not restricted to dewetting of thin films. Comparable structures can be found almost everywhere in nature [11]. It is known that the most stable polygon is a hexagon and the number of edges joined to a given vertex is 3. In our case it might sometimes be difficult to see the edges because the length of an edge can be shorter than the diameter of one droplet and thus might be invisible on the micrograph. Nevertheless, one can deduce from the micrographs that the most often found polygon is a hexagon and the vertices join three edges. The nearly regular size of the polygons is facilitated by the fact that at early stages when two small holes coalesce they do not necessarily form droplets at their contact line. The matter of the contact line is removed and a larger hole is formed. Thus very small polygons are not found. Droplet formation seems to require a hole of a certain minimal size.

The experiments described above show that dewetting of thin films proceeds via three stages: First, the films break up thus creating randomly distributed holes. Second, the holes then grow and the rims ahead of the holes eventually merge forming cellular structures. Third, the resulting ribbons are unstable and decay into droplets. The dependence of the average distance between initial holes on h^2 as well as the apparently simultaneous creation of the holes is in agreement with theoretical predictions invoking dewetting via spinodal decomposition. But there are at least two important questions unanswered. What is the detailed mechanism creating almost regular patterns although the initial holes are distributed randomly? How do the surface modulations evolve before the film breaks up? These and other problems will be tackled by future investigations.

The author is very grateful to A. Silberberg and A. Halperin for continuous encouragement and guidance in a field new to him at the beginning. He is also thankful to F. Brochard-Wyart for providing preprints of her work and helpful correspondence. Financial support by BMFT is acknowledged.

[1] A. Karim, A. Mansour, G. P. Felcher, and T. P. Russell, Phys. Rev. B **42**, 6846 (1990); G. Reiter and U. Steiner, J. Phys. II (France) **1**, 659 (1991).
[2] R. A. L. Jones *et al.*, Europhys. Lett. **12**, 41 (1990).
[3] D. J. Srolovitz and S. A. Safran, J. Appl. Phys. **60**, 247 (1986).
[4] K. Sekimoto, R. Oguma, and K. Kawasaki, Ann. Phys. (N.Y.) **176**, 359 (1987).
[5] W. F. Cooper and W. H. Nuttall, J. Agricult. Sci. **7**, 219 (1915).
[6] P.-G. de Gennes, Rev. Mod. Phys. **57**, 827 (1985).
[7] J. Daillant, J. J. Bennatar, and L. Leger, Phys. Rev. A **41**, 1963 (1990).
[8] F. Brochard-Wyart and J. Daillant, Can. J. Phys. **68**, 1084 (1990).
[9] F. Brochard-Wyart, J.-M. di Meglio, and D. Quéré, C. R. Acad. Sci. (Paris), Ser. II, **304**, 553 (1987).
[10] C. Redon, F. Brochard-Wyart, and F. Rondelez, Phys. Rev. Lett. **66**, 715 (1991).
[11] D. Weiare and N. Rivier, Contemp. Phys. **25**, 59 (1984).
[12] J. Stavans, E. Domany, and D. Mukamel, Europhys. Lett. **15**, 479 (1991).
[13] For the present experiments extremely smooth and homogeneous surfaces which are nonwettable for polystyrene are required. The actual composition of the surface is not crucial. The wafers are essentially equal except for a thin (< 1 nm) "contamination" layer which differs and is most probably due to different storage conditions after polishing. The wafers have been used as delivered. Only dust particles have been removed using wipes immersed in acetone.
[14] M. Foster, M. Stamm, G. Reiter, and S. Hüttenbach, Vacuum **41**, 1441 (1990).
[15] T. Young, Philos. Trans. R. Soc. London **95**, 65 (1805).
[16] G. Reiter (to be published).
[17] This rather high temperature and long time was chosen to make sure that the equilibrium situation is reached.
[18] Lord Rayleigh, Proc. London Math. Soc. **10**, 4 (1878).
[19] F. A. Nichols, and W. W. Mullins, Trans. Metall. Soc. AIME **233**, 1840 (1965).
[20] B. V. Deryagin, Kollidn. Zh. **17**, 191 (1955).

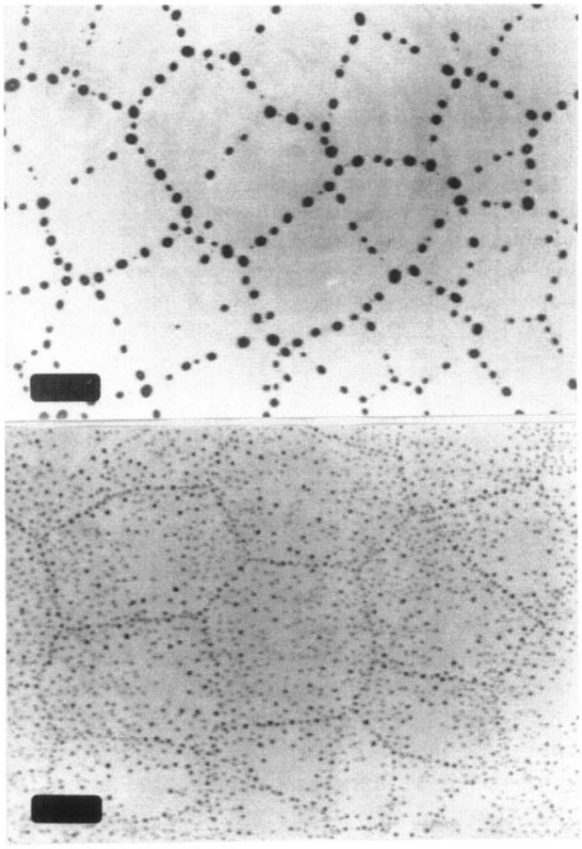

(a)

(b)

FIG. 1. Micrographs of the final stage of dewetting of 45-nm-thick polystyrene films on silicon wafers of (a) type *A* and (b) type *B*. The length of the bar is 100 μm.

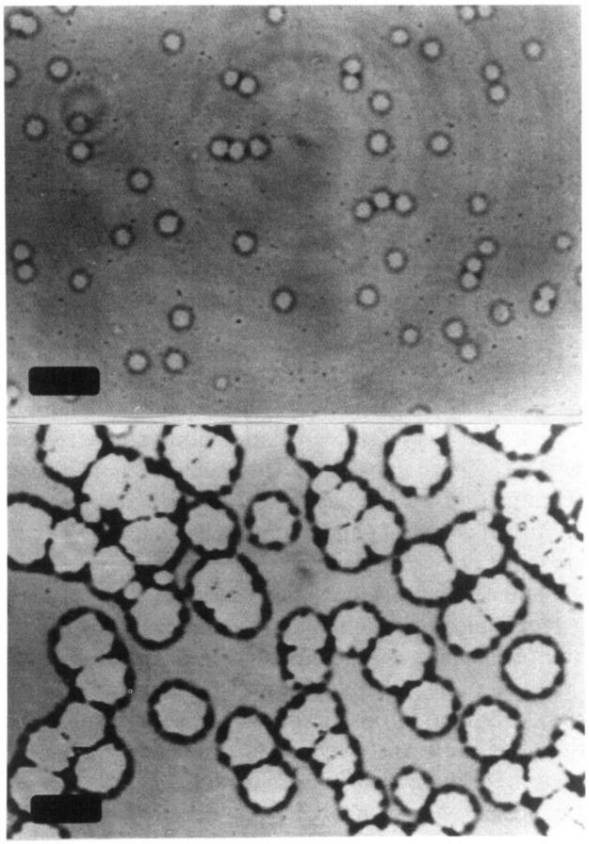

FIG. 2. Micrographs at different stages of dewetting of a 40.5-nm-thick polystyrene film on a silicon wafer of type *A* after (a) 20 min at 146 °C and (b) 120 min at 146 °C. The area between the holes has become rough during annealing as indicated by black spots on the micrographs [especially (a)]. The length of the bar is 100 μm.